

CEBAF Program Advisory Committee Eight Cover Sheet

This proposal must be received by close of business on Thursday, April 14, 1994 at:

CEBAF
User Liaison Office, Mail Stop 12 B
12000 Jefferson Avenue
Newport News, VA 23606

Proposal Title

The Electric Form Factor of the Neutron extracted from the ${}^3\text{He}(\vec{e}, e'n)\text{pp}$ Reaction

Contact Person

Name: W. Korsch & R. McKeown
Institution: Caltech
Address: Kellogg Radiation Laboratory 106-38
Address:
City, State ZIP/Country: Pasadena, California 91125
Phone: 818-395-4316 **FAX:** 818-564-8708
E-Mail → Internet: BMCK@erin.caltech.edu - KORSCH@erin.caltech.edu

Experimental Hall: A
Total Days Requested for Approval: 42
Minimum and Maximum Beam Energies (GeV): 4.0
Minimum and Maximum Beam Currents (μAmps): 15

CEBAF Use Only

Receipt Date: 4/14/94 PR 94-021

By: [Signature]

CEBAF Proposal

The Electric Form Factor of the Neutron extracted from the ${}^3\bar{\text{H}}\text{e}(\bar{e}, e'n)pp$ Reaction

B. Filippone, W. Korsch (co-spokesman), A. Lung, R. McKeown (co-spokesman), M. Pitt
California Institute of Technology, Pasadena, CA 91101

B. Anderson, G.G. Petratos, J. Watson
Kent State University, Kent, OH 44242

G.D. Cates, K. Kumar, P. Bgorad, H. Middleton
Princeton University, Princeton, NJ 08544

P.A. Souder, R. Holmes, J. McCracken, X. Wang
Syracuse University, Syracuse, NY 13210

L. Auerbach, J. Martoff, Z.-E. Meziani
Temple University, Philadelphia, PA 19122

I. Physics Motivation

Electron scattering has already been used for decades to measure the form factors of the proton and the neutron. The proton electric and magnetic form factors as well as the neutron magnetic form factor have been measured to high precision for Q^2 values up to several GeV^2/c^2 . However, our knowledge about the electric form factor of the neutron is quite unsatisfactory. This quantity is of fundamental theoretical interest, since it can serve as test for QCD based calculations. It is known from neutron-electron scattering that the slope of G_E^n is positive at $Q^2=0$, which implies an internal charge distribution of the neutron. So far most of the existing data on G_E^n were obtained from elastic and quasielastic scattering off deuterons. Here the model dependence of G_E^n on the deuteron wave functions is a fundamental limit for these kind of measurements. As polarized ^3He targets have become available for nuclear physics experiments, the neutron form factors can be extracted from asymmetry measurements, which are favourable over cross-section measurements, since the systematic uncertainties can be reduced significantly. Recently, a new series of measurements has been launched at different laboratories using polarized ^3He in inclusive and exclusive reactions to extract the electric and magnetic form factors of the neutron ([1]-[4]). There has also been a first attempt to extract G_E^n by measuring the (sideways) polarization transfer to the neutron in the $d(\vec{e}, e'\vec{n})p$ reaction [5]. This experiment allows in principle a direct way of extracting G_E^n in PWIA, when one stays in a kinematical regime where FSI and MEC contributions are kept small. However, one needs a well calibrated neutron analyzer system, to determine the polarization transfer to the neutron. This reduces the efficiency of the neutron detector. Several experiments have been proposed or already been performed to study the neutron spin structure in the deep inelastic regime. For example, the E142 collaboration at SLAC used polarized ^3He to extract the deep inelastic spin structure functions g_1^n and g_2^n of the neutron [6] whereas the SMC collaboration at CERN used deuterons for extracting the same quantities [7]. The HERMES collaboration is going to use both, ^3He and ^2H [8]. Since the knowledge of the structure of the neutron is of fundamental importance for nuclear physics, several nuclear probes should be used to study the form factors. Effects like medium modifications on the form factors are unknown in this kinematical regime and have to be studied in detail. The EMC effect is a good example that the influence of the surrounding medium can be sizeable. Therefore, we propose to measure G_E^n using a polarized ^3He target at three different values of the 4-momentum squared, namely Q^2

$= 1 \text{ GeV}^2/c^2, 1.5 \text{ GeV}^2/c^2, \text{ and } 2 \text{ GeV}^2/c^2.$

II. Discussion of the Experiment

We propose a set of measurements to determine the electric form factor of the neutron using the ${}^3\bar{\text{He}}(\bar{e}, e'n)pp$ reaction at three different values of Q^2 in Hall A at CEBAF. This method was first proposed by R. Arnold, C.E. Carlson, and F. Gross [9] as a polarization transfer experiment in the $d(\bar{e}, e'n)p$ reaction. Since dense polarized ${}^3\text{He}$ targets have become available the ${}^3\bar{\text{He}}(\bar{e}, e'n)pp$ reaction can also be used for the extraction of G_E^n . The ${}^3\bar{\text{He}}$ nucleus serves here as a polarized neutron. The advantage of extracting G_E^n via the ${}^3\bar{\text{He}}(\bar{e}, e'n)pp$ reaction is that one does not have to measure the polarization of the neutron in the exit channel. The efficiency of the neutron detector is therefore higher. We want to extract G_E^n for Q^2 values of 1.0, 1.5, and 2.0 GeV^2/c^2 . The scattered electrons will be detected in one of the high resolution spectrometers (HRS) and for neutron detection we plan to build an array of 4 layers of scintillator material (NE-102) with a total active area of $60 \times 60 \text{ cm}^2$ and a thickness of about 10 cm per layer (total thickness 40 cm). The active area would be divided into 3 segments of 20 cm each. We expect to achieve a neutron detection efficiency ϵ of about 5% per layer which amounts to about 20 % in the total efficiency. The neutron detector will be built by our collaborators from KSU [10] and detailed design work is still in progress.

The measured asymmetry for the ${}^3\bar{\text{He}}(\bar{e}, e'n)pp$ reaction can be expressed as follows in PWIA:

$$A = -P_e P_n D \left\{ \frac{2\sqrt{\tau(\tau+1)} \tan(\vartheta_e/2) G_E^n G_M^n \sin(\theta^*) \cos(\phi^*)}{G_E^n{}^2 + G_M^n{}^2(\tau + 2\tau(1+\tau) \tan^2(\vartheta_e/2))} + \frac{2\tau\sqrt{1+\tau + (1+\tau)^2 \tan^2(\vartheta_e/2)} \tan(\vartheta_e/2) G_M^n{}^2 \cos(\theta^*)}{G_E^n{}^2 + G_M^n{}^2(\tau + 2\tau(1+\tau) \tan^2(\vartheta_e/2))} \right\}. \quad (1)$$

Here P_e is the electron polarization, P_n is the neutron polarization, D a dilution factor (see below), $\tau = (Q^2/4 m_n^2)$, ϑ_e is the electron scattering angle, G_E^n and G_M^n are the neutron electric and magnetic form factors, respectively, θ^* is the polar angle of the ${}^3\text{He}$ spin vector relative to the q_3 vector, and ϕ^* is the azimuthal angle of the target spin

vector relative to the scattering plane. The dilution factor is due to the fact that the target contains nitrogen and rubidium besides ^3He . Presently we assume a ^3He volume density of about $2.5 \cdot 10^{20}$ atoms/cm³, the Rb density will be of the order $6 \cdot 10^{14}$ /cm³, and the nitrogen partial pressure will about 100 torr or $1.4 \cdot 10^{19}$ N/cm³ at room temperature. These numbers combined amount in a dilution factor of 0.94, which is the ratio of the total number of ^3He neutrons to the total number of neutrons in the target. Eqn. 1 shows the obvious sensitivity to G_E^n in the longitudinal-transversal interference term. Therefore, by aligning the target spin perpendicular to \vec{q} , i.e. choosing $\theta^* = 90^\circ$, and $\phi^* = 0^\circ$ the above equation can be rewritten in the following form:

$$G_E^n = -\frac{A_{perp}}{P_e P_n D} \cdot \frac{G_M^n (\tau + 2\tau(1 + \tau) \tan^2(\vartheta_e/2))}{2\sqrt{\tau(1 + \tau) \tan(\vartheta_e/2)}}. \quad (2)$$

Aligning the target spin parallel to \vec{q} reduces Eqn 2 to ($G_E^n \approx 0$):

$$A_{long} = -P_e P_n D \frac{2\sqrt{1 + \tau + (1 + \tau)^2 \tan^2(\vartheta_e/2)} \tan(\vartheta_e/2)}{1 + 2(1 + \tau) \tan^2(\vartheta_e/2)}. \quad (3)$$

This equation is completely independent of the neutron form factors and serves as an excellent calibration reaction. Combining Equations 2 and 3 gives

$$G_E^n = \sqrt{\tau + \tau(1 + \tau) \tan^2(\vartheta_e/2)} \frac{A_{perp}}{A_{long}} G_M^n. \quad (4)$$

In principal Eqn.2 as well as Eqn.4 can be used to extract G_E^n , but it is obvious that the systematic error which is attached to Eqn.4 is smaller than in Eqn.2. Therefore we want to use Eqn.4 to extract G_E^n , especially, since it will be shown that A_{long} can be measured to a good precision in a relatively short time. Table 1 lists the values for G_E^n in Galster parameterization [11], G_M^n in dipole parameterization, and the expected perpendicular asymmetries for our three Q^2 values.

The estimates for the reaction rates were performed with a Monte Carlo code which is a modified version of the EGN code developed by van den Brand [12]. The cross-sections were calculated in PWIA with de Forest's CC1 off-shell description [13] and the ^3He wave function generated by Schulze and Sauer [14]. We used a pointlike target in

TABLE 1 G_E^n in Galster parameterization, G_M^n in dipole parameterization, and A_{perp} for the proposed values of Q^2 . A beam polarization of 0.8, a target polarization of 0.45, (i.e. a neutron polarization of 0.39), and a dilution factor of 0.94 has been applied to A_{perp} . See text for details.

| Q^2 [GeV ² /c ²] | G_E^n | G_M^n | A_{perp} |
|--|----------------------|---------|------------------------|
| 1.0 | $3.61 \cdot 10^{-2}$ | 0.329 | $-1.716 \cdot 10^{-2}$ |
| 1.5 | $2.48 \cdot 10^{-2}$ | 0.197 | $-2.125 \cdot 10^{-2}$ |
| 2.0 | $1.78 \cdot 10^{-2}$ | 0.131 | $-2.408 \cdot 10^{-2}$ |

our calculation. The acceptances of the HRS are ± 30 mr in the horizontal plane and ± 65 mr in the vertical plane. The total solid angle for the electron arm is therefore 7.8 msr. The momentum acceptance $\Delta p/p$ of the HRS is 10% and the transverse length acceptance is 10 cm. As mentioned above the neutron detector will have an active area of 60×60 cm² with a total neutron detection efficiency of about 0.2. The detector will be positioned about 7.80 m away from the target at a Q^2 of 1 GeV²/c² and about 10 m away for the Q^2 values of 1.5 and 2.0 GeV²/c². This ensures that we have enough timing resolution (≈ 1 ns) to distinguish between quasielastically scattered neutrons and neutrons associated with pion production. The solid angle is about 6 msr for the low Q^2 value and 3.6 msr for the two higher Q^2 . The solid angle is purposely kept small (up to about 50 MeV/c transverse momentum), to keep the background low and to keep the kinematics close to the quasielastic peak. In order to distinguish charged particles from the neutrons, we will add thin ΔE scintillators in front of the the neutron detector. In addition we will install a Pb wall to suppress low energetic electromagnetic background. The additional dilution in the asymmetry due to (p,n) reactions in the target window and shielding walls will be studied in "background" runs. Experience at Mainz shows that the loss in the neutron flux can be up to 40% due to the Pb shielding. Therefore, we assumed a total neutron detection efficiency of $0.2 \cdot 0.6 = 0.12$.

We assume a beam current of $15 \mu A$ electrons with a beam polarization of 80%. Such high beam polarizations have been already achieved at SLAC with quantum efficiencies of 0.1-0.3 %. The target polarization will be about 45 %. For detailed information see

the section on the target. Table 2 lists some experimental parameters.

TABLE 2 Experimental parameters for the three different Q^2 settings at an incident beam energy of 4 GeV. The effective target length was taken to be $10\text{cm}/\sin(\vartheta_e)$.

| Q^2 [GeV ² /c ²] | ϑ_e [°] | ϑ_q [°] | E' [GeV] | eff. tgt. length [cm] | tgt. density [cm ⁻²] |
|--|----------------------|----------------------|---------------|--------------------------|-------------------------------------|
| 1.0 | 15.5 | 54.3 | 3.463 | 37.4 | $9.4 \cdot 10^{21}$ |
| 1.5 | 20 | 47.1 | 3.182 | 29.2 | $7.3 \cdot 10^{21}$ |
| 2.0 | 24 | 41.8 | 2.923 | 24.6 | $6.1 \cdot 10^{21}$ |

Based on these assumptions we get counting rates and accuracies as shown in Table 3.

TABLE 3 Estimated rates and accuracies for the perpendicular asymmetry. We assume a ³He polarization of 0.45, a beam polarization of 0.8, a dilution factor of 0.94, and a neutron detection efficiency ϵ of 0.12.

| Q^2 [GeV ² /c ²] | Rate [s ⁻¹] | Rate· ϵ [s ⁻¹] | N_{tot} (10 days) | $\Delta A = \frac{1}{\sqrt{N}}$ (10 days) | $\frac{\Delta A}{A_{perp}}$ [%] |
|--|----------------------------|--|---------------------|---|------------------------------------|
| 1.0 | 30.3 | 3.6 | $3.11 \cdot 10^6$ | $5.67 \cdot 10^{-4}$ | 3.3 |
| 1.5 | 3.2 | 0.38 | $3.28 \cdot 10^5$ | $1.75 \cdot 10^{-3}$ | 8.0 |
| 2.0 | 0.84 | 0.10 | $8.64 \cdot 10^4$ | $3.40 \cdot 10^{-3}$ | 13.7 |

Similarly, Table 4 displays the longitudinal asymmetry for $G_E^n = 0$.

If we assume the following relative accuracies for the beam energy: $5 \cdot 10^{-4}$, the scattered electron energy: $1 \cdot 10^{-4}$, G_M^n : 0.05 [15], and if further the electron scattering angle is known to ± 2 mr, we will end up with a total systematic error of about 5%. It is clear that the systematic error is dominated by the error in G_M^n . Systematic errors in the determination of beam - and target polarizations cancel since we use the

TABLE 4 Estimated rates and accuracies for the longitudinal asymmetry. Same assumptions as in Table 3

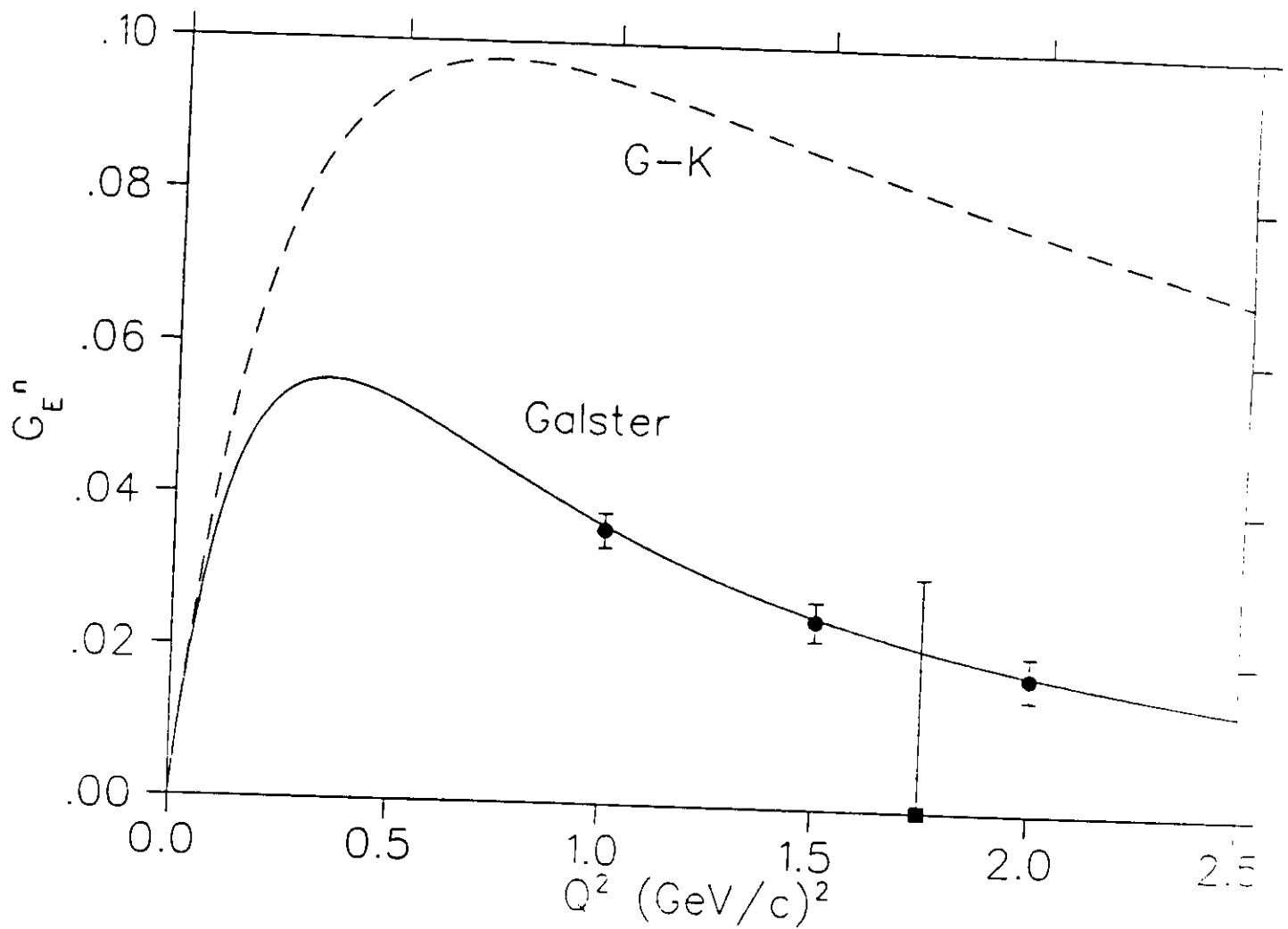
| Q^2 [GeV ² /c ²] | τ | ϑ_e [°] | N_{tot} (1 day) | A_{long} [%] | $\frac{\Delta A}{A_{long}}$ (1 day) [%] |
|--|--------|----------------------|-------------------|-------------------|--|
| 1.0 | 0.286 | 15.5 | $3.11 \cdot 10^5$ | - 8.77 | 2.0 |
| 1.5 | 0.435 | 20.0 | $3.28 \cdot 10^4$ | - 11.64 | 4.7 |
| 2.0 | 0.573 | 24.0 | $8.64 \cdot 10^3$ | - 14.20 | 7.6 |

ratio A_{perp}/A_{long} for extracting G_E^n . The total projected errors in the extraction of G_E^n are listed in Table 6 and Fig. 1 shows the error bars as compared to the Galster parameterization of G_E^n .

TABLE 6 Total fractional errors for the extraction of G_E^n . Here the G_E^n values in the Galster parameterization were used.

| Q^2 [GeV ² /c ²] | $\frac{\Delta G_E^n}{G_{E Galster}^n}$ [%] |
|--|---|
| 1.0 | ± 6.3 |
| 1.5 | ± 10.5 |
| 2.0 | ± 16.4 |

FIGURE 1 G_E^n as a function of Q^2 . The solid curve corresponds to the Galster parameterization. Shown are the projected error bars of the proposed experiment as well as the data point from Lung et al. [15]



III. The Polarized ^3He Target

The polarized target will be based on the principle of spin exchange between optically pumped alkali-metal vapor and noble-gas nuclei ([16], [17], [18]). The design will be similar in many ways to that used in E-142, an experiment at SLAC to measure the spin dependent structure function of the neutron [19]. A central feature of the target will be sealed glass target cells, which will contain a ^3He pressure of about 10 atmospheres. As indicated in Fig. 2, the cells will have two chambers, an upper chamber in which the spin exchange takes place, and a lower chamber, through which the electron beam will pass. In order to maintain the appropriate number density of alkali-metal (which will probably be Rb) the upper chamber will be kept at a temperature of 170-200°C using an oven constructed of the high temperature plastic Torlon. With a density of 2.5×10^{20} atoms/cm³, and a lower cell length of 40 cm, the target thickness will be 1.0×10^{22} atoms/cm².

We describe below in greater detail some features of the target.

Operating Principles

The time evolution of the ^3He polarization can be calculated from a simple analysis of spin-exchange and ^3He nuclear relaxation rates [20]. Assuming the ^3He polarization $P_{^3\text{He}} = 0$ at $t = 0$,

$$P_{^3\text{He}}(t) = \langle P_{\text{Rb}} \rangle \left(\frac{\gamma_{\text{SE}}}{\gamma_{\text{SE}} + \Gamma_{\text{R}}} \right) \left(1 - e^{-(\gamma_{\text{SE}} + \Gamma_{\text{R}}) t} \right) \quad (5)$$

where γ_{SE} is the spin-exchange rate per ^3He atom between the Rb and ^3He , Γ_{R} is the relaxation rate of the ^3He nuclear polarization through all channels other than spin exchange with Rb, and $\langle P_{\text{Rb}} \rangle$ is the average polarization of a Rb atom. Likewise, if the optical pumping is turned off at $t = 0$ with $P_{^3\text{He}} = P_0$, the ^3He nuclear polarization will decay according to

$$P_{^3\text{He}}(t) = P_0 e^{-(\gamma_{\text{SE}} + \Gamma_{\text{R}}) t} \quad (6)$$

The spin exchange rate γ_{SE} is defined by

$$\gamma_{\text{SE}} \equiv \langle \sigma_{\text{SE}} v \rangle [\text{Rb}]_{\text{A}} \quad (7)$$

where, $\langle \sigma_{SE} v \rangle = 1.2 \times 10^{-19} \text{ cm}^3/\text{sec}$ is the velocity-averaged spin-exchange cross section for Rb- ^3He collisions ([20], [21], [22]) and $[\text{Rb}]_A$ is the average Rb number density seen by a ^3He atom. Our target will be designed to operate with $1/\gamma_{SE} = 8$ hours.

From Eq. (6) it is clear that there are two things we can do to get the best possible ^3He polarization — maximize γ_{SE} and minimize Γ_R . But from Eq. (7) it is also clear that maximizing γ_{SE} means increasing the alkali-metal number density, which in turn means more laser power. The number of photons needed per second must compensate for the spin relaxation of Rb spins. In order to achieve $1/\gamma_{SE} = 8$ hours, we will require about 24 Watts of usable laser light at a wavelength of 795 nm. We will say more about the source of laser light below.

The rate at which polarization is lost, which is characterized by Γ_R , will have four principle contributions. An average electron beam current of about 15 μA will result in a depolarization rate of $\Gamma_{\text{beam}} = 1/30$ hours [23]. Judging from experience at SLAC, we can produce target cells with an intrinsic rate of $\Gamma_{\text{cell}} = 1/50$ hours. This has two contributions, relaxation that occurs during collisions of ^3He atoms due to dipole-dipole interactions [24], and relaxation that is presumably due largely to the interaction of the ^3He atoms with the walls. Finally, relaxation due to magnetic field inhomogeneities can probably be held to about $\Gamma_{\nabla B} = 1/100$ hours [25]. Collectively, under operating conditions, we would thus expect

$$\Gamma_R = \Gamma_{\text{beam}} + \Gamma_{\text{cell}} + \Gamma_{\nabla B} = 1/30 \text{ hours} + 1/50 \text{ hours} + 1/100 \text{ hours} = 1/16 \text{ hours} . \quad (8)$$

Thus, according to Eq. 5, the target polarization cannot be expected to exceed

$$P_{\text{max}} = \frac{\gamma_{SE}}{\gamma_{SE} + \Gamma} = 0.66 . \quad (9)$$

Realistically, we will not achieve a Rb polarization of 100% in the pumping chamber, which will reduce the polarization to about 45-50%.

Target Cells

The construction and filling of the target cells must be accomplished with great care if $1/\Gamma_{\text{cell}}$ is to be in excess of 50 hours. We plan to use the "Princeton Prescription" which was developed for use in SLAC E-142. This resulted, among the cells that were tested, in lifetimes that were always better than 30 hours, and in about 60% of the cells, better than 50 hours. The following precautions will be taken:

1. Cells will be constructed from aluminosilicate glass.
2. All tubing will be "resized." This is a process in which the diameter of the tubing is enlarged by roughly a factor of two in order to insure a smooth pristine glass surface that is free of chemical impurities.
3. Cells will be subjected to a long (4-7 day) bake-out at high ($> 400^{\circ}\text{C}$) temperature on a high vacuum system before filling.
4. Rb will be doubly distilled in such a manner as to avoid introducing any contaminants to the system.
5. The ^3He will be purified either by getters or a liquid ^4He trap during filling.

The cells will be filled to a high density of ^3He by maintaining the cell at a temperature of about 20 K during the filling process. This is necessary so that the *pressure* in the cell is below one atmosphere when the glass tube through which the cell is filled is sealed.

The length of the cell has been chosen to be 40 cm so that the end windows will not be within the acceptance of the Hall A spectrometers. The end windows themselves will be about $100\ \mu$ thick. Thinner windows could in principle be used, but this does not appear to be necessary.

The Optics System

As mentioned above, approximately 20-24 Watts of "usable" light at 795 nm will be required. By "usable," we essentially mean light that can be readily absorbed by the Rb. It should be noted that the absorption line of the Rb will have a full width of several hundred GHz at the high pressures of ^3He at which we will operate. Furthermore, since we will operate with very high Rb number densities that are optically quite thick, quite a bit of light that is not within the absorption linewidth is still absorbed.

It is our plan to take advantage of new emerging diode laser technology to economically pump the target. Systems are now commercially available in which a single chip produces about 20 watts of light, about half of which is probably usable. Between 2-4 such systems, at a cost of about \$25,000 each, should do the job. There is also a group at Lawrence Livermore Laboratory that has offered to build us a single chip that can produce 150 watts. While some studies of the use of diode lasers for spin-exchange optical pumping do exist in the literature [26], actual demonstrations of high polarizations in cells suitable for targets are much more recent [27]. It is our opinion that diode lasers will probably work, but we will perform several tests before freezing this decision.

At SLAC, five titanium-sapphire/argon ion laser systems were used to drive the E-142 polarized ^3He target. This option will definitely work, but is much more expensive.

Polarimetry

Polarimetry will be accomplished by two means. During the experiment, polarization will be monitored using the NMR technique of adiabatic fast passage (AFP) [28]. The signals will be calibrated by comparing the ^3He NMR signals with those of water. The calibration will be independently verified by studying the frequency shifts that the polarized ^3He nuclei cause on the electron paramagnetic resonance (EPR) lines of Rb atoms [23]. This second technique will be performed in separate target studies, not during the experiment. It will serve solely as a check of our calibration. We plan to determine the polarization of the target to within 5% of itself.

Apparatus Overview

The target will be in air or, perhaps, in a helium bag. This greatly simplifies the design. The main components of the target are shown in Fig. 2.

The "main coils" shown are large Helmholtz coils that will be used to apply a static magnetic field of about 20 Gauss. In addition to establishing the quantization axis for the target, the main coils are important for suppressing relaxation due to magnetic field inhomogeneities, which go like $1/B^2$. At 20 G, inhomogeneities can be as large as about 30 mG/cm while keeping $\Gamma_{\nabla B} < 1/100$ hours. By increasing the applied field to about 40 G, and relaxing our requirements on $\Gamma_{\nabla B}$ by about a factor of two, inhomogeneities as large as 0.25 G/cm can be tolerated. We are still finalizing our final choice of static field.

The NMR components in the target include a set of RF drive coils, and a separate set of pick-up coils. Not shown in the figure are the NMR electronics, which include an RF power amplifier, a lock-in amplifier, some bridge circuitry, and the capability to sweep the static magnetic field.

The oven shown in Fig. ?? is constructed of Torlon, a high temperature plastic. The oven is heated with forced hot air.

The optics system will either include five Ti:sapphire lasers (only one is shown) or 2-4 laser diode systems. Either way, there will also be several lenses and a quarter wave plate to provide circular polarization.

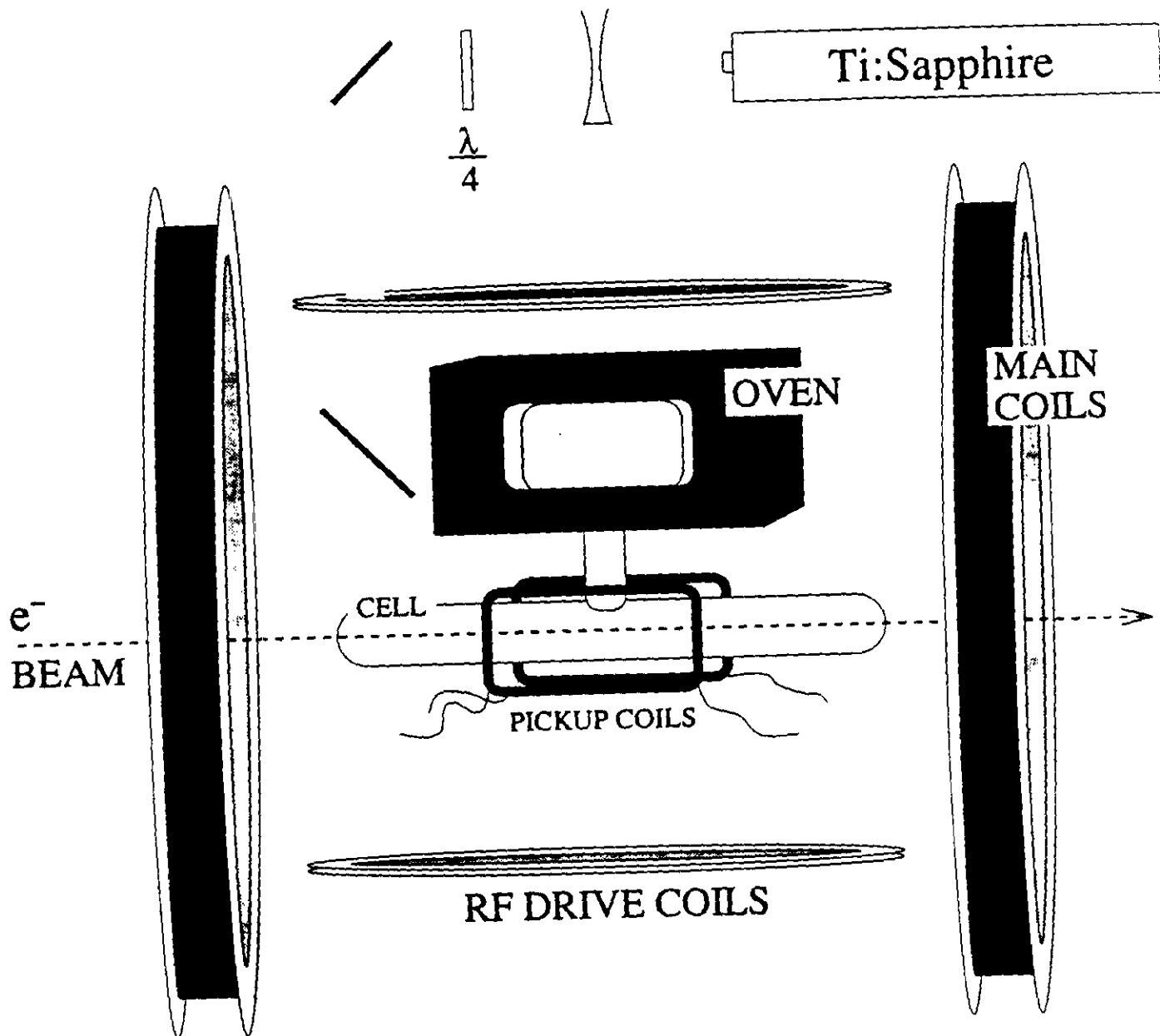


Figure 2

IV. Contribution of the Collaboration and Beam Time Request

It has been shown in the previous chapters that the ${}^3\bar{\text{H}}\text{e}(\bar{e}, e'n)pp$ reaction is a very powerful tool to extract G_E^n . The contribution of the collaboration to the experiment will be:

- Construction and installation of the polarized ${}^3\text{He}$ target. This includes Helmholtz coils for the target guiding field and target polarimeter.
- Construction of the neutron detector.

We request from CEBAF:

- Polarized beam of $15\mu\text{A}$ and a beam polarization of 80% at a beam energy of 4 GeV.
- Support for target installation.
- Beam pipe instrumentation, i.e. beam position and beam current monitors.
- Working polarimeter to measure the beam polarization.
- Neutron detector shielding.

(We would like to note that this experiment only requires that 1 HRS spectrometer be operational in Hall A.)

Further we request a total running time of 1000 hrs to perform the complete experiment. We will need 800 hrs for the production run, about 70 hrs for beam polarization measurements (about 2 hours per day), 10% of the data taking for background studies, i.e. 80 hrs, and 50 hrs for moving of the spectrometers and neutron detector with shielding.

V. References

- [1] J.L. Friar *et al.*, Phys. Rev. **C42**, 2310 (1990).
- [2] H. Gao *et al.*, "Measurement of the neutron magnetic form factor from inclusive quasielastic scattering of polarized electrons from polarized ^3He ", submitted to Phys. Rev. Lett. (1994).
- [3] C.E. Jones *et al.*, Phys. Rev. **C47**, 110, (1993).
- [4] T.E. Chupp *et al.*, Phys. Rev. **C45**, 915, (1992).
- [5] M. Meyerhof *et al.*, "First measurement of the electric formfactor of the neutron in the exclusive scattering of polarized electrons from polarized ^3He ", Mainz preprint
- [6] P.L. Anthony *et al.* (E142 Collaboration), Phys. Rev. Lett. **71**, 959 (1993).
- [7] B. Adeva *et al.* (SMC Collaboration), Phys. Lett. **B302**, 533 (1993).
- [8] The HERMES Collaboration, Proposal to measure the spin-dependent structure functions of the neutron and the proton at HERA.
- [9] R.G. Arnold *et al.*, Phys. Rev. **C23**, 363 (1981).
- [10] "Neutron Detection Systems for CEBAF", J.W. Watson, Research Program at CEBAF (III) (1987).
- [11] S. Galster *et al.*, Nucl. Phys. **B32**, 221 (1971).
- [12] J.v.d. Brand, private communication.
- [13] T. de Forest, Nucl. Phys. **A392**, 232 (1983).
- [14] R.-W. Schulze and P.U. Sauer, Phys. Rev. **C48**, 38, (1993).
- [15] A. Lung *et al.*, Phys. Rev. Lett. **70**, 718 (1993).
- [16] M.A. Bouchiat, T.R. Carver and C.M. Varnum, Phys. Rev. Lett. **5**, 373 (1960).
- [17] N.D. Bhaskar, W. Happer, and T. McClelland. Phys. Rev. Lett. **49**, 25 (1982).
- [18] W. Happer, E. Miron, S. Schaefer, D. Schreiber, W.A. van Wijngaarden, and X. Zeng, Phys. Rev. A **29**, 3092 (1984).
- [19] P. L. Anthony *et al.*, Phys. Rev. Lett. **71**, 959 (1993).
- [20] T.E. Chupp, M.E. Wagshul, K.P. Coulter, A.B. McDonald, and W. Happer, Phys. Rev. C **36**, 2244 (1987).
- [21] K.P. Coulter, A.B. McDonald, W. Happer, T. E. Chupp, and M.E. Wagshul, Nuc. Inst. Meth. in Phys. Res. A **270**, 90 (1988).

- [22] N.R. Newbury, A.S. Barton, P. Bogorad, G. D. Cates, M. Gatzke, H. Mabuchi, and B. Saam, *Phys. Rev. A* **48**, 558 (1993).
- [23] K.P. Coulter, A.B. McDonald, G.D. Cates, W. Happer, T.E. Chupp, *Nuc. Inst. Meth. in Phys. Res.* **A276**, 29 (1989).
- [24] N. R. Newbury, A. S. Barton, G. D. Cates, W. Happer, and H. Middleton, *Phys. Rev. A* **48**, 4411 (1993).
- [25] G.D. Cates, S.R. Schaefer and W. Happer, *Phys. Rev. A* **37**, 2877 (1988); G.D. Cates, D.J. White, Ting-Ray Chien, S.R. Schaefer and W. Happer, *Phys. Rev. A* **38**, 5092 (1988).
- [26] M. E. Wagshul and T. E. Chupp, *Phys. Rev. A* **40**, 4447 (1989).
- [27] Private communication, Bill Cummings (1994).
- [28] A. Abragam, *Principles of Nuclear Magnetism* (Oxford University Press, New York, 1961).